Optical constants of the as-prepared and annealed $(Se_{80}Te_{20})_{94}Ag_6$/PMMA thin films

A. Gupta[a,b,*], K. Malik[c], R. Kumar[d]
[a]*Department of Physics, Gurukula Kangri Vishwavidyalaya, Haridwar, India*
[b]*Department of Applied Sciences and Humanities, ABES Engineering College, Ghaziabad, India*
[c]*Department of Applied Sciences and Humanities, BBDIT, Ghaziabad, India*
[d]*Garg Degree College, Laksar, Haridwar, India*

Thin films of $(Se_{80}Te_{20})_{94}Ag_6$/PMMA have been deposited on glass substrate by thermal co-evaporation technique. Melt quenching approach has been adopted to prepared bulk $(Se_{80}Te_{20})_{94}Ag_6$ chalcogenide glass. Glass transition temperature of bulk $(Se_{80}Te_{20})_{94}Ag_6$ glass and poly (methyl methacrylate) (PMMA) polymer have been found out by differential scanning calorimetry (DSC) at a heating rate of 10 K/min. Thin films were annealed above glass transition temperatures of glass (332 K) and polymer (340 K) at two different temperatures 343 K and 365 K. The presence of different phases in annealed film was confirmed by X-ray diffraction studies. Transmission spectra of as-deposited and annealed films were obtained by Uv-Vis spectroscopy in the wavelength range of 350-900 nm. To analyze refractive index dispersion Wemple-Didomenico model have been used. Optical parameters viz refractive index (n), extinction coefficient (k), real and imaginary dielectric constants (ε′ and ε′′) and optical band gap (E_g) are calculated by using optical transmittance. The increasing behavior of the optical band gap with increase in annealing temperature is explained on the basis of density of state model.

(Received June 1, 2021; Accepted September 22, 2021)

Keywords: Thermal co-evaporation, Glass transition temperature, Transmission spectra, Refractive index dispersion, Annealing temperature

1. Introduction

The chalcogenide glassy alloy having Se-Te as constituent materials are used in many electronic devices. The addition of third element Ag is supposed to make some disorder in comparison to the binary alloys. The properties of these materials like low phonon energy, good chemical durability, high refractive index and high photosensitivity attracts the researchers towards them for further investigation about their optical, electrical & thermal properties [1]. The addition of Ag has a great effect on the electrical behavior [2] which increases the d.c. conductivity and decreases the activation energy. The glass forming regions in which the glasses show a tendency to crystallize forms the basis for memory switches [3-5]. The transformation of amorphous state to crystalline state can be used in recording & removing the information in context to chalcogenide glasses.

Poly (methyl methacrylate) (PMMA) is one of the most useful amorphous polymer of acrylate family. PMMA is an optically transparent thermoplastic amorphous material [6]. Due to its light weight, high mechanical strength, high resistance to shatter and scratch and ease in processing, PMMA is used as replacement of inorganic glasses. It has refractive index 1.49 and shows excellent optical properties [7]. PMMA with chalcogenide glasses has great potential in developing a Bragg's Stack for the application of gas sensing. A Lalova1 et al. have prepared Bragg stack from $As_{30}Ge_{10}S_{60}$/PMMA, As_2S_3/PMMA and three layered As_2S_3/PMMA/As_2S_3 structure as a gas-sensing applications in the IR spectral range. The potential application of the chalcogenide glasses/PMMA films are also in the field of 1D photonic crystal used as optical sensor [8-11]. M. Y. Shubar et al. have studied the optical nonlinearities in the Binary

* Corresponding author: anubha.gupta@abes.ac.in
https://doi.org/10.15251/CL.2021.189.549

Bi_2S_3/PMMA and Bi_2Te_3/PMMA films for the application in optical switching devices [12-14]. D. Nayak et al. have studied the optical and electrical properties of ZnS/PMMA system as the emissive layer for organic light emitting diode application [15]. Keeping in mind the above discussion, we have prepared thin films of SeTeAg glass/PMMA polymer by thermal co-evaporation method. In the present work we have studied the effect of annealing on some optical properties like optical band gap, refractive index, extinction coefficient and dielectric constant of $(Se_{80}Te_{20})_{96}Ag_6$/PMMA Thin films.

2. Experimental

$(Se_{80}Te_{20})_{96}Ag_6$ glassy sample was prepared by melt quenching technique. Selenium, tellurium and silver constituents of high purity were taken in their atomic weight ratio. These constituents were sealed in highly evacuated glass ampoule. The ampoule was placed in rocking furnace. Rocking procedure was done continuously at 950 ^oC for 24 hours to get homogeneous melt of constituents. To quench the melt, ampoule was quickly dropped in ice cold water. To study the glass transition temperature and crystallization temperature, differential scanning calorimetry (DSC) (Shimadzu TA-60) has been carried out for the bulk glassy sample and poly (methyl methacrylate) (PMMA) separately. For DSC scan approximately 10 mg of fine power was sealed in alumina pan and heated at constant heating rate 10 K/min in nitrogen atmosphere. Thin films of SeTeAg glass/PMMA polymer were formed by thermally co-evaporation of constituents by vacuum coating unit. Two different evaporation sources of $(Se_{80}Te_{20})_{96}Ag_6$ and PMMA have been used to deposit thin film at a pressure of 10^{-5} Torr. Thin films were deposited on a prior cleaned glass substrate. Thin films were annealed in the presence of a nitrogen atmosphere at two different temperatures 343K and 365 K for 2 hours. Annealing temperatures were selected higher than the glass transition temperature of glass and polymer. To prevent oxidation of the sample the annealing was done in a vacuum in the atmosphere of nitrogen gas. Wavelength dependent optical transmittance $T(\lambda)$ of as-prepared and annealed thin films was measured using Uv-VIS spectrophotometer (Shimadzu UV-Viz-NIR 3600) in the 350-900 nm range. Optical transmittance was utilized to determine optical parameter viz. band gap, extinction coefficient and dielectric constant of the material.

3. Results and discussion

Differential scanning calorimetery (DSC) has been carried out for $(Se_{80}Te_{20})_{94}Ag_6$ glass and PMMA polymer at constant heating rates 10 K/min. In the fig. 1 the first exothermic peak represents the glass transition temperature. From the DSC scan the glass transition temperature of glass and polymer are found to be 332 K and 340 K respectively. Thermally co-evaporated $(Se_{80}Te_{20})_{94}Ag_6$ glass and PMMA polymer are used to deposit thin film in the ratio of 1:1 weight percent. We have deposited three films out of which two films were annealed, one at 343K and the other at 365 K. The annealing process was done in vacuum under the flow of nitrogen gas for two hours. Fig. 2 represents the X-ray diffraction pattern of annealed $(Se_{80}Te_{20})_{94}Ag_6$/PMMA film at temperature 365 K. Different crystalline phases are identified as Te, Se_8, Ag_2Se and Ag_2Te in the annealed film [16].

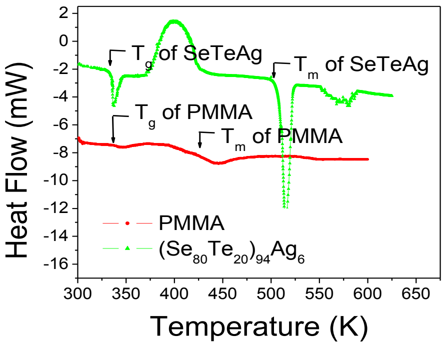

Fig.1. DSC thermogrammes of $(Se_{80}Te_{20})_{94}Ag_6$ glasses and PMMA polymer.

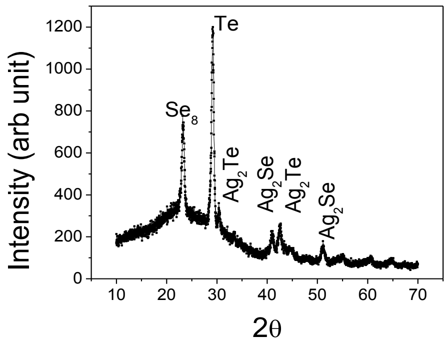

Fig.2. X-ray diffraction pattern of $(Se_{80}Te_{20})_{94}Ag_6$/PMMA thin film annealed at 365 K.

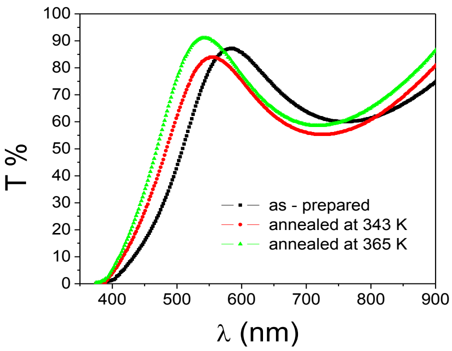

Fig.3. Transmittance of $(Se_{80}Te_{20})_{94}Ag_6$/PMMA thin films.

The normal incidence transmittance of as-prepared and annealed thin films has been recorded by Uv-Vis spectroscopy in the 350 - 900 nm wavelength range. These transmission spectra have been used to calculate optical constants such as refractive index (n), extinction coefficient (k), real and imaginary parts of dielectric constants (ε′ and ε″) and optical band gap (E_g) by using the following relations. The relations suggested by Swanepoel [17-19], have been used for determining the refractive index.

$$n = \sqrt{N + \sqrt{N^2 - s^2}} \tag{1}$$

where

$$N = \frac{2s}{T_{min}} - \frac{(s^2 + 1)}{2} \tag{2}$$

$$N = 2s\,\frac{T_{max} - T_{min}}{T_{max}\,T_{min}} + \frac{(s^2 + 1)}{2} \tag{3}$$

where T_{max} is the envelope function of the transmittance maxima.

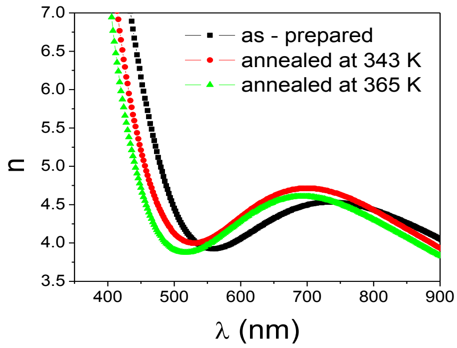

Fig.4. Refractive index of $(Se_{80}Te_{20})_{94}Ag_6$*/PMMA thin films.*

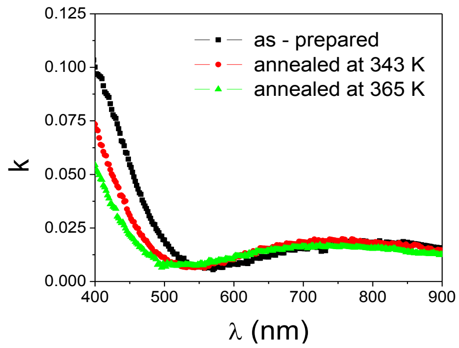

Fig.5. Extinction coefficient of $(Se_{80}Te_{20})_{94}Ag_6$*/PMMA thin films.*

The thickness of the film can be calculated by the following relation

$$d = \frac{\lambda_1\,\lambda_2}{2\,(\lambda_1\,n_2 - \lambda_2\,n_1)} \tag{4}$$

where λ_1 and λ_2 are the wavelengths corresponding to refractive indices of two consecutive maxima n_1 or minima n_2.

The extinction coefficient k was calculated by

$$k = \frac{\lambda}{4\,\pi\,d}\,\ln\left(\frac{1}{x}\right) \tag{5}$$

where x is the absorbance and may be given as

$$x = \frac{E_M - \sqrt{E_M^2 - (n^2-1)^3\,(n^2 - s^2)}}{(n^2-1)^3\,(n^2 - s^2)} \tag{6}$$

and

$$E_M = \frac{8n^2 s}{T_{max}} + (n^2 - 1)(n^2 - s^2) \tag{7}$$

The absorption coefficient (α) was calculated from the following relation

$$\alpha = \frac{4\pi k}{\lambda} \tag{8}$$

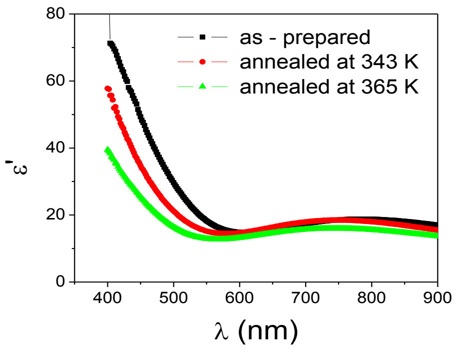

Fig.6. Variation of real dielectric constant with wavelength in $(Se_{80}Te_{20})_{94}Ag_6$/PMMA thin films.

Table 1. Optical parameters such as refractive index (n), Extinction coefficient (k), real and imaginary dielectric constants (ε′ and ε″) at 500 nm wavelength and optical band gap (E_g).

Samples	n	k	ε′	ε″	E_g (eV)
As-Prepared	4.32	0.018	30.36	0.152	2.51
Annealed at 343K	4.13	0.011	21.19	0.088	2.56
Annealed at 365 K	3.77	0.007	16.27	0.058	2.60

The real and imaginary dielectric constants of investigated films have been calculated by using the relation (9) and (10) respectively [20].

$$\varepsilon' = n^2 - k^2 \tag{9}$$

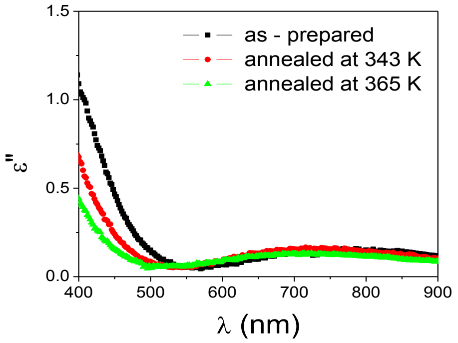

Fig.7. Variation of imaginary dielectric constant with wavelength in $(Se_{80}Te_{20})_{94}Ag_6$/PMMA thin films.

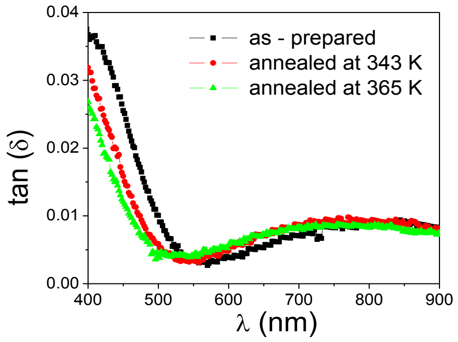

Fig.8. Variation of dielectric loss with wavelength in $(Se_{80}Te_{20})_{94}Ag_6$/PMMA thin films.

$$\varepsilon'' = 2\,n\,k \tag{10}$$

And dissipation factor, tan δ may be expressed as

$$\tan\delta = \frac{\varepsilon''}{\varepsilon'} \tag{11}$$

From the Table 1it is found that the values of real and imaginary dielectric constants are decreasing with increases in annealing temperature. The decrease in ε′ and ε″ values indicate the decrease in density of defects states [21].

The refractive index dispersion was analyzed by using the Wemple-Didomenico’s dispersion model. According to a single-oscillator model (Wemple-DiDomenico model) [22-24] the relation between the refractive index *n*, and photon energy *h*ν, may be written as follows

$$n^2(h\nu) = 1 + \frac{E_0\,E_d}{E_0^2-(h\nu)^2} \tag{12}$$

where *h*ν is the photon energy, E_0 is the oscillator energy and E_d is the oscillator strength or dispersion energy. The oscillator energy E_0, is an average energy gap, can be obtained by using Eq.12. Fig. 9 shows the linear fits of $(n^2-1)^{-1}$ Vs $(h\nu)^2$ for annealed and un-annealed films. The values of WDD dispersion parameters, E_0 and E_d, for all the films, were determined directly from the slope $(E_0E_d)^{-1}$, and the intercept (E_0/E_d) of the straight lines, are shown in Table 1. The values of the static refractive index n_0 (the zero-frequency refractive index) of studied films were calculated from WDD dispersion parameters E_0 and E_d by using a formula

$$n_0 = \left(1+\frac{E_d}{E_0}\right)^{\frac{1}{2}} \tag{13}$$

Table 2. Oscillator energy (E_o), dispersion energy (E_d) and static refractive index (n_0) of $(Se_{80}Te_{20})_{94}Ag_6$/PMMA films at wavelength 500 nm.

Samples	E_0	E_d	n_0
As-Prepared	5.27	3.16	1.63
Annealed at 343K	5.06	3.29	1.59
Annealed at 365 K	4.59	3.32	1.54

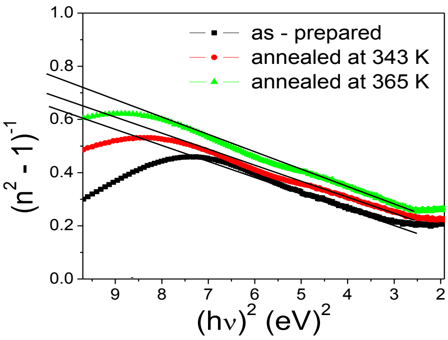

Fig.9. Variation of $(n^2 - 1)^{-1}$ with $(h\nu)^2$ in $(Se_{80}Te_{20})_{94}Ag_6$/PMMA thin films.

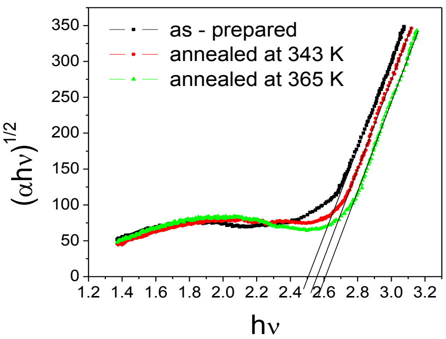

Fig.10. Variation of $(\alpha h\nu)^{1/2}$ with hν in $(Se_{80}Te_{20})_{94}Ag_6$/PMMA thin films.

The optical band gap of as-prepared and annealed films is determined by using Tauc's relation [25].

$$\alpha h\nu = B\,(h\nu - E_g)^2 \tag{14}$$

where B is constant, which is a measure of the extent of band tailing.

The values of band gap are determined from the intercept on the energy axis from the graph drawn between $(\alpha h\nu)^{1/2}$ and hν. The calculated values of band gap for as-prepared, annealed at 343K and 365K are 2.51, 2.56 and 2.60eV respectively. It is observed that value of band gap goes on increasing with increase in annealing temperature. X-ray analysis of annealed films confirms that different phases are generated in the annealed film. The increasing behavior of band gap energy with annealing temperature can be explained by density of states model given by Mott and Davis [26]. This model suggests that in the amorphous glassy materials a large number of defects states are produced in the gap. During the deposition of films a lot of dangling bonds and defects are generated in the films. Annealing above glass transition temperature removes defects and saturates the unsaturated bonds as a result, defects states are minimized in the gap leading to increase in the band gap.

4. Conclusions

Glass transition temperature of bulk $(Se_{80}Te_{20})_{94}Ag_6$ glass and PMMA have been evaluated by DSC. Transmission spectra of the films have been taken out before and after heat treatment in the wavelength range 350-900 nm. X-ray diffraction study of annealed film of $(Se_{80}Te_{20})_{94}Ag_6$/PMMA reveals that the film has different phases under annealing. The band gap is going on increasing with increase in annealing temperature. The increasing behavior in band gap is explained on the basis of Davis and Mott's model.

References

[1] N. Kushwaha, V. S. Kushwaha, R. K. Shukla, A. Kumar, J. Non-Cryst. Solids **351**, 3414 (2005).
[2] M. Mirandou, M. Fontana, B. Arcondo, J. Mater. Process. Technol.**143-144**, 420 (2003).
[3] J. A. Savage, J. Mater Sci.**7**, 64 (1972).
[4] S. C. Moss, J. P. Deneufville, Mater. Res. Bull. **79**, 423 (1972).
[5] V. Vassilev, S. Parvanov, T. Hristova-Vasileva, V. Parvanova, D. Ranova, Mater. Chem. Phys. **105**, 53 (2007).
[6] J. W. Lamb, Int. J. infrared millim. waves, **17**(12), 1997 (1996).
[7] A. H. Charles, M. P. Edward, Plastics Materials and processes, in concise Encyclopedia, Wiley: NJ, 42 (2003).
[8] A. Lalova, R. Todorov, Bulg. Chem. Commun.**45** (B), 59 (2013).
[9] A. Lalova, R. Todorov, J. Phys. Conf. Ser. **514**, 012014 (2014).
[10] A. Lalova, R. Todorov, Bulg. Chem. Commun. **47**(B), 29 (2015).
[11] T. Babeva, G. Marinov, J. Tasseva, A. Lalova, R. Todorov, J. Phys. Conf. Ser. **398**, 012025 (2012).
[12] M. Y. Shubar, H. L. Saadon, S. J. Abbas, J. Phys. Conf. Ser.**1234**, 012059 (2019).
[13] M.Y. Shubar, H. L. Saadon, S. J. Abbas, Mater. Technol. **35**(8), 494 (2019).
[14] M. Y. Shubar, H. L. Saadon, S. J. Abbas, Chin. Opt. Lett. **18**(1), 011902 (2020).
[15] D. Nayak, R. B. Choudhary, Opt. Mater. **91**, 470 (2019).
[16] D. Singh, S. Kumar, R. Thangraj, J. Non-Cryst. Solids, **358**, 2826 (2012).
[17] R. Swanepoel, J. Phys. E Sci. Instrum. **17**, 896 (1984).
[18] R. Swanepoel, J. Phys. E Sci. Instrum. **16**, 1224 (1983).
[19] J. C. Manifacier, J. Gasiot, J. P. Fillard, J. Phys. E Sci.Instrum.**9**, 1002 (1976).
[20] M. M. Wakkad, E. Kh. Shoker, S. H. Mohamed, J. Non-cryst. Solids **265**, 157 (2000).
[21] D. Singh, S. Kumar, R. Thangaraj, T. S. Sathiaraj, Physica B **408**, 119 (2013).
[22] S. Wemple, M. diDominnico Jr, Phys. Rev. B1, 193 (1970).
[23] S. H. Wemple, M. diDomineco, Phys. Rev. B**3**, 1338 (1971).
[24] S. H. Wemple, Phys. Rev. B**7**, 3767(1973).
[25] J. Tauc, Optical properties of amorphous semiconductors, Amorphous & liquid semiconductors, Ed., Springer US, 159 (1974).
[26] N. F. Mott, E. A. Davis, Electronics Processes in Non-Crystalline Materials, 2nd edn. Clarendon Press, Oxford, UK, (1979).